The EMBO Journal vol.13 no.1 pp.42-53, 1994

VIP21/caveolin, glycosphingolipid clusters and the sorting of glycosylphosphatidylinositol-anchored proteins in epithelial cells

Chiara Zurzolo[1,3], Wouter van't Hof[1], Gerrit van Meer[2] and Enrique Rodriguez-Boulan[1,4]

[1]Department of Cell Biology and Anatomy, Cornell University Medical College, 1300 York Avenue, New York, USA and
[2]Department of Cell Biology, University of Utrecht Medical School, AZU H02.314, Heidelberglaan 100, 3584 CX Utrecht, The Netherlands
[3]Present address: Dipartimento di Biologia e Patologia Cellulare e Molecolare, CEOS, CNR, II Policlinico, Via Pansini 5, 80131 Napoli, Italy
[4]Corresponding author

Communicated by P.De Camilli

We studied the role of the association between glycosylphosphatidylinositol (GPI)-anchored proteins and glycosphingolipid (GSL) clusters in apical targeting using gD1-DAF, a GPI-anchored protein that is differentially sorted by three epithelial cell lines. Differently from MDCK cells, where both gD1-DAF and glucosylceramide (GlcCer) are sorted to the apical membrane, in MDCK Concanavalin A-resistant cells (MDCK-ConA^r) gD1-DAF was mis-sorted to both surfaces, but GlcCer was still targeted to the apical surface. In both MDCK and MDCK-ConA^r cells, gD1-DAF became associated with TX-100-insoluble GSL clusters during transport to the cell surface. In dramatic contrast with MDCK cells, the Fischer rat thyroid (FRT) cell line targeted both gD1-DAF and GlcCer basolaterally. The targeting differences for GSLs in FRT and MDCK cells cannot be accounted for by a differential ability to form clusters because, in spite of major differences in the GSL composition, both cell lines assembled GSLs into TX-100-insoluble complexes with identical isopycnic densities. Surprisingly, in FRT cells, gD1-DAF did not form clusters with GSLs and, therefore, remained completely soluble. This clustering defect in FRT cells correlated with the lack of expression of VIP21/caveolin, a protein localized to both the plasma membrane caveolae and the trans Golgi network. This suggests that VIP21/caveolin may have an important role in recruiting GPI-anchored proteins into GSL complexes necessary for their apical sorting. However, since MDCK-ConA^r cells expressed caveolin and clustered GPI-anchored proteins normally, yet mis-sorted them, our results also indicate that clustering and caveolin are not sufficient for apical targeting, and that additional factors are required for the accurate apical sorting of GPI-anchored proteins.
Key words: epithelia/glycosphingolipid/GPI-anchored proteins/sorting/VIP21-caveolin

Introduction

In simple epithelia, the protein and lipid composition of the apical plasma membrane differs from that of the basolateral membrane, which is the basis for their different vectorial transport functions (Rodriguez-Boulan and Nelson, 1989; Simons and Wandinger-Ness, 1990). The apical membrane has an unusually high concentration of glycolipids which may protect the epithelial cell from the frequently harsh environment faced by the apical surface (Simons and van Meer, 1988). Similarly, membrane proteins anchored to the bilayer by the glycophospholipid glycosylphosphatidylinositol (GPI) (Ferguson and Williams, 1988; Low and Saltiel, 1988; Cross, 1990) have been found polarized to the apical membrane in several epithelial cell lines (Lisanti *et al.*, 1988, 1990a; Wilson *et al.*, 1990) and to the bile canaliculi, the apical pole of hepatocytes (Ali and Evans, 1990). The apical targeting role of GPI is supported by the expression in MDCK cells of GPI-anchored proteins, either native ones (Powell *et al.*, 1991) or recombinant chimeras of basolateral proteins with bona fide GPI-anchoring signals (Brown *et al.*, 1989; Lisanti *et al.*, 1989), which resulted in the apical targeting and localization of these proteins.

The apical enrichment of both glycosphingolipids (GSLs) and GPI-anchored proteins has been shown to result from sorting in the Golgi apparatus and vectorial apical delivery (van Meer and Simons, 1988; Lisanti *et al.*, 1990b; van't Hof and van Meer, 1990). It is also known that certain GSLs tend to form tight clusters when they constitute a high molar fraction of the bilayer lipids (Thompson and Tillack, 1985). Based on this property, van Meer and Simons have proposed that association with GSL rafts may be a key event in the sorting of apical proteins (van Meer and Simons, 1988; Simons and Wandinger-Ness, 1990). This model, referred to here as the 'cluster hypothesis', received support from experiments by Skibbens *et al.* (1989), who showed that an apical protein, influenza HA, became insoluble in TX-100 at the time that it migrated through the trans Golgi network (TGN) in MDCK cells. Additional support for this hypothesis was provided by the recent observation (Brown and Rose, 1992) that an exogenous GPI-anchored protein, placental alkaline phosphatase (PLAP), became insoluble in TX-100 at low temperature, as it reached the *cis*-Golgi of MDCK cells. Interestingly, the detergent-insoluble aggregates of PLAP were enriched in sphingomyelin (SM), cholesterol and GSLs. Because GSLs are produced in the Golgi apparatus (van Meer and Burger, 1992; van Meer, 1993), this provides additional evidence that clusters of GPI-anchored proteins and GSLs are formed in this organelle before being transported to the cell surface.

However, biophysical evidence suggests that clustering is not sufficient for apical localization (Hannan *et al.*, 1993). In MDCK cells, a fusion GPI-anchored protein, gD1-DAF, was found to reach the apical surface forming part of clusters that were relatively immobile, presumably because of interaction with the sorting machinery. In contrast, a Concanavalin A resistant (ConA^r) mutant of MDCK cells that cannot sort GPI-anchored proteins, failed to immobilize the clusters of gD1-DAF, suggesting that a component of

the sorting machinery is altered in this cell line. Furthermore, clustering, as detected by detergent insolubility, is not exclusive to epithelial cells and, therefore, cannot by itself be the sole mechanism responsible for apical sorting (reviewed by Brown, 1992; Rodriguez-Boulan and Powell, 1992).

The data on the mobility of GPI-anchored proteins in MDCK cells suggest that these proteins are clustered before reaching the cell surface. This is also supported by their resistance to dissociation, at steady state, by certain mild non-ionic detergents (TX-100, Triton X-114) at low temperature (Hoessli and Rungger-Brandle, 1985; Hooper and Turner, 1988). In addition, GPI-anchored proteins have been found concentrated in surface caveolae, small invaginated pits or vesicles with a diameter of ~50 nm. These vesicles are coated cytoplasmically by delicate filaments with a major protein component of 22 kDa, caveolin (Rothberg *et al.*, 1992). Interestingly, a protein identical to caveolin, VIP21, has been isolated from MDCK cells in association with post-TGN apical and basolateral vesicles (Kurzchalia *et al.*, 1992) and in the TGN (Dupree *et al.*, 1993). This suggests that VIP21/caveolin may share similar functions at both the plasma membrane and the TGN (Dupree *et al.*, 1993).

The Fischer rat thyroid (FRT) cell line provides an excellent model to study the relationship between clustering with GSLs and sorting of GPI-proteins. Whereas these cells display similar polarity to MDCK cells with respect to the distribution of apical and basolateral transmembrane proteins (Zurzolo *et al.*, 1992a; Zurzolo and Rodriguez-Boulan, 1993), including several viral glycoproteins (Zurzolo *et al.*, 1992b), they differ from MDCK cells in that they sort GPI-anchored proteins preferentially to the basolateral surface (Zurzolo *et al.*, 1993). Thus, like MDCK-ConA^r cells, FRT cells behave as a 'mutant' cell line with respect to GPI-protein localization. In this report, we show that the basolateral localization of GPI-anchored proteins in FRT cells is accompanied by their inability to be incorporated into detergent-insoluble aggregates with GSLs and by the basolateral delivery of a GSL. This 'clustering defect' of FRT cells correlates with the absence of VIP21/caveolin. In addition, we show that in MDCK-ConA^r cells the GPI-anchored proteins do cluster and that caveolin is present. These results suggest that VIP21/caveolin plays an important role in the clustering of GPI-anchored proteins, but also indicate that additional adaptor proteins may be required for their apical targeting.

Results

GPI and sphingolipid sorting in MDCK, FRT and MDCK-ConA^r cells

GPI-anchored proteins have been shown to be distributed preferentially to the apical membrane of MDCK and other epithelial cell lines (Lisanti *et al.*, 1988, 1990a,b). Two exceptions to this pattern have been observed: one is found in FRT cells, which sort GPI proteins to the basolateral membrane (Zurzolo *et al.*, 1993), and the second is in MDCK-ConA^r cells, which cannot sort GPI proteins in any biased pattern (Lisanti *et al.*, 1990a). In this study, we have chosen MDCK, FRT and MDCK-ConA^r cells as model cell lines to study the differences in the sorting mechanisms of GPI-anchored proteins. As a marker protein, we utilized a

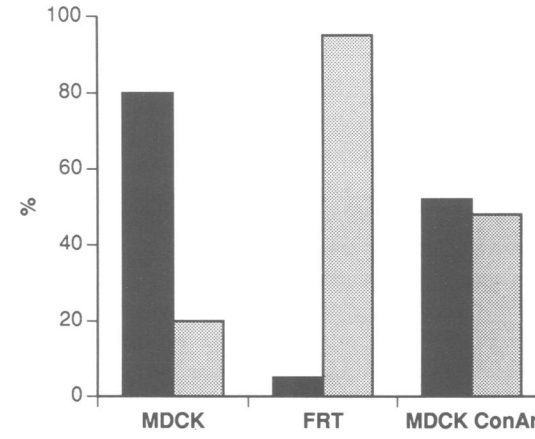

Fig. 1. Delivery of gD1−DAF in transfected MDCK, FRT and MDCK-ConA^r cells. Surface amino groups of 5-day-old filter-grown monolayers were quenched with six consecutive rounds of sulfo-SHPP. Cells were then warmed at 37°C for 90 min and subjected to apical or basolateral biotinylation. The monolayers were extracted and immunoprecipitated with anti-HSV IgG and run on SDS−PAGE. Biotinylated proteins were revealed with [^{125}I]streptavidin blotting/autoradiography. Fluorograms of two independent experiments were quantitated and the results expressed as percent apical (black bars) and percent basolateral (gray bars) surface expression of gD1−DAF in stably expressing clones.

fusion protein between the ectodomain of gD1 (the native glycoprotein of herpes simplex virus) and the GPI attachment signals for DAF (decay accelerating factor), gD1−DAF, which was permanently expressed by transfection in the different cell lines. To quantify the polarized surface delivery of newly synthesized gD1−DAF in transfected MDCK, FRT and MDCK-ConA^r cells, we used a biotin targeting assay (Lisanti *et al.*, 1988) with cells that were grown on polycarbonate filters for 4 or 5 days (Figure 1). In accordance with previous results (Lisanti *et al.*, 1989; Zurzolo *et al.*, 1993), we found that gD1−DAF was preferentially delivered to the apical membrane of MDCK cells (80−85% after 90 min chase), and to the basolateral membrane (>95%) in FRT cells. In MDCK-ConA^r cells, the delivery to the cell surface was not polarized, which explains its non-polarized surface distribution (Lisanti *et al.*, 1990a; Hannan *et al.*, 1993).

Using various sphingolipid analogs, it was previously shown that a newly synthesized GSL glucosylceramide (GlcCer), was preferentially targeted to the apical domain of MDCK and Caco-2 cells, when compared with the phospholipid SM (van Meer *et al.*, 1987; van't Hof and van Meer, 1990; van't Hof *et al.*, 1992). A current hypothesis proposes that co-clustering of GPI-anchored proteins and GSLs may be important for their sorting to the apical domain of epithelial cells (van Meer and Simons, 1988; Lisanti and Rodriguez-Boulan, 1990; Brown, 1992). The anomalous sorting of GPI-anchored proteins in FRT and MDCK-ConA^r cells prompted us to analyze GSL sorting in these cells, using *N*-6-[7-nitro-2,1,3-benzodiaxole-4-yl]amino-hexanoyl(C6-NBD)-ceramide as a probe. After incorporation of the ceramide precursor at low temperature, delivery to the cell surface of two intracellularly synthesized products, C6-NBD-GlcCer and C6-NBD-SM, was monitored at 37°C by exchange with bovine serum albumin (BSA). The polarity of each sphingolipid was defined as the apical/basolateral ratio of delivery. The quotient of these ratios, the relative

Table I. Sphingolipid sorting in MDCK, FRT and MDCK-ConA^r cells

Cell line	Polarity GlcCer (ap/bl)	Polarity SM (ap/bl)	Relative polarity (sorting)	[*n*]
MDCK	1.9 ± 0.2	0.9 ± 0.2	2.2 ± 0.3	3
FRT	0.22 ± 0.06	0.50 ± 0.10	0.44 ± 0.03	5
MDCK-ConA^r	3.8 ± 0.4	1.8 ± 0.3	2.1 ± 0.2	4

polarity GlcCer/SM, was used as a measure of 'sorting' of GlcCer from SM (van't Hof and van Meer, 1990). In agreement with previous results (van Meer *et al.*, 1987), MDCK cells showed a 2-fold apical enrichment of GlcCer relative to SM (Table I). In MDCK-ConA^r cells, although the polarities of delivery for each lipid were higher, the same sorting of GSL as in MDCK cells was observed. Interestingly, in FRT cells the numbers both for the polarities of delivery and for lipid sorting were exactly reversed, resulting in a 2-fold basolateral enrichment of GlcCer as compared with SM (Table I).

Different TX-100 extractability of newly synthesized gD1–DAF in MDCK, FRT and MDCK-ConA^r cells

GPI-anchored proteins have been reported to be insoluble in TX-100 (Hoessli and Rungger-Brandle, 1985; Hooper and Turner, 1988). Insolubilization occurs during the biosynthetic transport from the endoplasmic reticulum (ER) to the early Golgi or at the *cis*-Golgi, and has been suggested to be an indication of clustering of GPI proteins with GSL-rich patches (Brown and Rose, 1992). Using a pulse–chase protocol, we examined the insolubilization of gD1–DAF in TX-100 during biosynthesis in MDCK, FRT and MDCK-ConA^r cells. In MDCK cells, gD1–DAF was almost completely soluble in TX-100 at the earliest time of chase (Figure 2A), and it became progressively more insoluble in the detergent during the chase time. After 3 h, ~50% of the protein was resistant to extraction by TX-100. Note that the insolubility was acquired before the terminal glycosylation of the protein, as detected by the increase in the molecular weight of the protein during the chase (Figure 2A). This suggested that gD1–DAF becomes insoluble before it reaches the medial Golgi cisternae. These results are in agreement with those from Brown and Rose (1992), who showed that PLAP becomes insoluble in the early Golgi in MDCK cells. The extent of TX-100 insolubilization of these two proteins is different, probably reflecting intrinsic differences between the two proteins (Hooper and Turner, 1988). Remarkably, the same assay repeated in FRT cells gave a completely different result (Figure 2B): gD1–DAF remained totally soluble in TX-100 at all times of the chase. In contrast, gD1–DAF showed similar behavior in MDCK-ConA^r cells as in MDCK cells (Figure 2C): after 3 h chase ~35–40% of the protein was insoluble in TX-100 (Figure 2C). As in MDCK cells, the protein became insoluble before reaching the surface, presumably at an early point in the transport pathway.

The insolubilization of gD1–DAF was specific for TX-100. When the same assay was performed using octylglucoside or CHAPS, gD1–DAF was found to be completely soluble in all three cell lines (data not shown). Additionally, when we performed the extraction in TX-100 at 4°C for 5 min instead of the usual 20 min, we did not find any difference in the extractability of gD1–DAF in any of the cell lines (data not shown), indicating that we did not use limiting conditions, insufficient to solubilize all the marker protein.

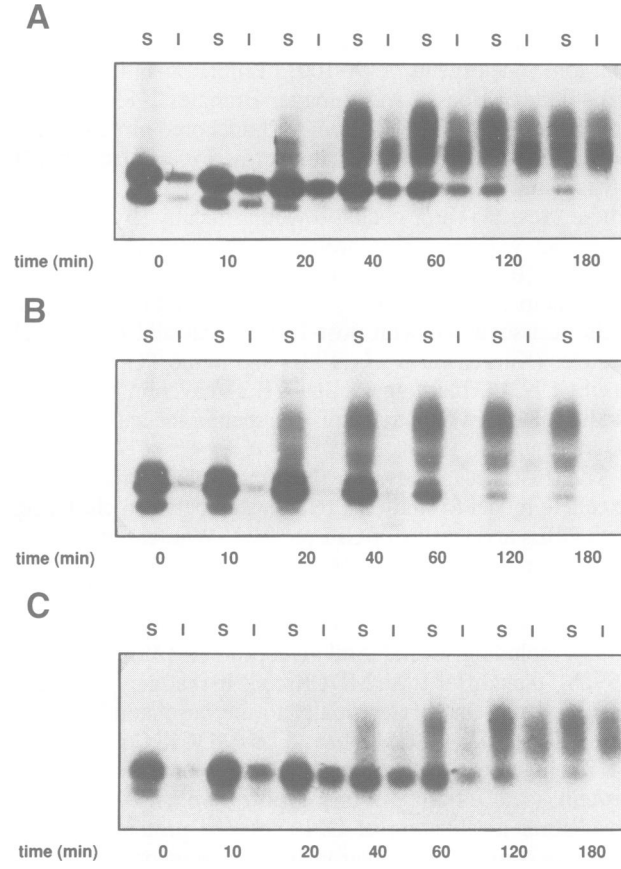

Fig. 2. Pulse–chase analysis of gD1–DAF solubility in TX-100. MDCK, FRT and MDCK-ConA^r cells stably expressing gD1–DAF were grown to confluency and pulsed for 5 min (as described in Materials and methods), followed by incubation in chase medium for the indicated times. After 20 min extraction in TNE/TX-100 buffer at 4°C, both the soluble (S) and the insoluble (I) fractions were collected, and gD1–DAF was subsequently immunoprecipitated and analyzed by SDS–PAGE and fluorography. (**A**) MDCK; (**B**) FRT; (**C**) MDCK-ConA^r cells.

We also studied the TX-100 extractability of two apical transmembrane proteins, gp114 (Le Bivic *et al.*, 1990) and gp135 (Ojakian and Schwimmer, 1988) in MDCK cells (Figure 3A and B), and of an apical (DPPIV) and a basolateral (Ag35/40kD) transmembrane protein (Zurzolo *et al.*, 1992a) in FRT cells (Figure 3C). We found that both gp114 and gp135 were completely extractable in TX-100 during pulse–chase experiments in MDCK cells (Figure 3A and B). Similarly, DPPIV and Ag35/40kD were always soluble in FRT cells (Figure 3C). These results suggested that TX-100 insolubilization was relatively specific for GPI-anchored proteins, since no endogenous apical transmembrane protein was found to be insoluble in MDCK or FRT cells.

Lipid composition and resistance to TX-100 extraction in MDCK, FRT and MDCK-ConA^r cells

In MDCK cells, GPI-proteins become detergent insoluble in between the ER and early Golgi (Figure 2A), which is the major cellular location for synthesis of SM (Futerman *et al.*, 1990; Jeckel *et al.*, 1990). SM is one of the most detergent-insoluble lipids in MDCK cells (Brown and Rose, 1992) and has also been proposed to play a role in directing biosynthetic transport of cholesterol (van Meer, 1989), another lipid found in TX-100-insoluble residues in MDCK cells. To gain understanding of the differential sorting and detergent solubility of gD1−DAF, we decided to compare the phospholipid compositions of MDCK, FRT and MDCK-ConA^r cells (Table II). Total phospholipids were analyzed according to Bligh and Dyer (1959), separated by two-dimensional HPTLC, and quantified. No significant differences in the relative phospholipid compositions were observed among the three cell lines (Table II). We also analyzed the detergent extractability of the various phospholipids, including SM, using the same extraction conditions that we had used for gD1−DAF (20 min on ice in 1% TX-100). As observed before (Brown and Rose, 1992), SM was the most TX-100-resistant phospholipid (Table II). Although SM tended to be slightly more soluble in FRT cells, it was consistently 70−90% insoluble in MDCK, FRT and MDCK-ConA^r cells. We found no significant differences in the detergent extractability of the remaining phospholipids in the three cell lines. This indicates that the differential detergent insolubility of gD1−DAF is not related to differences in SM or phospholipid composition.

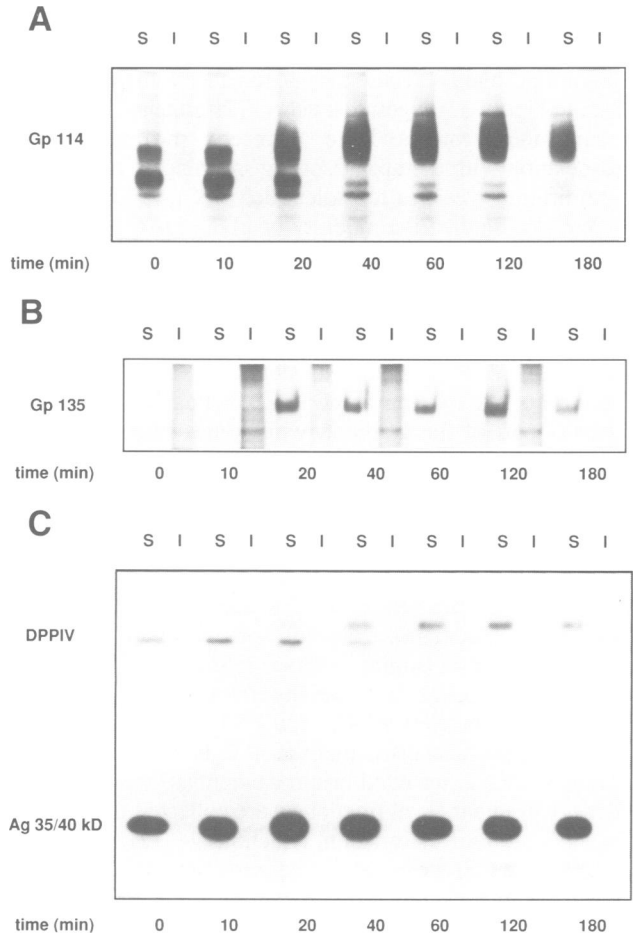

Fig. 3. Pulse−chase analysis of transmembrane protein solubility in TX-100. Two endogenous apical transmembrane proteins of MDCK cells, gp114 (**A**) and gp135 (**B**), and one apical and one basolateral protein from FRT cells, DPPIV and Ag35/40kD (**C**), were subjected to the same assay shown in Figure 2. Note that all four proteins, in both MDCK and FRT cells, are completely soluble at all chase times during their transport to the cell surface.

Next, we analyzed the composition of GSLs and their extractability in TX-100 in both MDCK and FRT cells, after labeling with [^{3}H]galactose. Following entry into the cell, [^{3}H]galactose is quickly converted into UDP-galactose and epimerized into glucose, thereby forming a general hexose donor that efficiently labels cellular GSLs (Saito *et al.*, 1984; van Echten and Sandhoff, 1989). After overnight labeling of MDCK and FRT cells, we observed prominent differences in the glycolipid patterns (Figure 4). The major products in MDCK cells were the neutral glycolipids GlcCer, GalCer, LacCer and Forssman antigen, and the acidic glycolipids sulfatide and GM_3, whilst several globosides were labeled as minor products. Relative to MDCK, FRT cells were characterized by a reduction in the galactose-containing glycolipids GalCer, LacCer, Forssman antigen and sulfatide. FRT cells essentially expressed GlcCer and the gangliosides GM_3 and GD_3, the last being absent in MDCK cells (Figure 4). These differences in the composition of radiolabeled GSLs were concluded to be representative for both cell lines by comparison with the total cold glycolipid compositions (data not shown) and by the fact that they were consistent over a time period of 2−16 h (data not shown).

Interestingly, after TX-100 extraction of [^{3}H]galactose-labeled cells, detergent-insoluble GSLs were observed in both MDCK and FRT cells (Figure 4). As measured by densitometric scanning of fluorographs from two separate experiments, the detergent insolubility was strikingly similar for the common GSLs: GlcCer was 40% and GM_3 was 50% insoluble. In MDCK cells, Forssman antigen was 75%

Table II. Phospholipid composition and TX-100 insolubility in MDCK, FRT and MDCK-ConA^r cells

	MDCK		FRT		MDCK-ConA^r	
	% Total phospholipid	% TX-100 insoluble	% Total phospholipid	% TX-100 insoluble	% Total phospholipid	% TX-100 insoluble
SM	6.2 ± 1.2	87.4 ± 5.5	8.8 ± 1.3	72.0 ± 10.4	7.0 ± 0.3	81.6 ± 3.8
PI	6.7 ± 1.5	13.0 ± 5.8			8.6 ± 0.1	20.0 ± 3.1
			17.3 ± 7.9[a]	32.9 ± 11.7[a]		
PS	5.7 ± 1.7	55.7 ± 24.7			5.9 ± 0.2	63.2 ± 12.2
PC	53.2 ± 8.7	12.2 ± 3.4	55.9 ± 3.3	12.8 ± 1.5	54.4 ± 5.1	12.1 ± 1.2
PE	28.1 ± 5.0	16.1 ± 6.0	17.9 ± 3.7	17.0 ± 3.0	28.5 ± 0.6	20.0 ± 1.2

PI, phosphatidylinositol; PS, phosphatidylserine; PC, phosphatidylcholine; PE, phosphatidylethanolamine
[a]PI + PS

insoluble, GalCer and LacCer 25−35%, and sulfatide was 45% insoluble, all in general agreement with previous observations (Brown and Rose, 1992). In FRT cells, the ganglioside GD_3 was 40% resistant. In contrast, globosides in both cell lines, and the small amount of LacCer in FRT, were almost completely solubilized by TX-100 (<10% resistant).

Insoluble gD1−DAF associates with GSLs

To determine whether gD1−DAF was associated with TX-100-insoluble GSLs, we examined the insoluble residue by centrifugation to equilibrium in sucrose density gradients. For these experiments we modified a protocol devised by Brown and Rose (1992). Briefly, the cells were pulsed for 20 min with [^{35}S]Met/Cys, incubated for 1 h in chase medium, and lysed in buffer containing 1% TX-100. The TX-100 lysates were adjusted to 40% sucrose and a linear gradient (5−30% sucrose) was layered on top. This was subjected to centrifugation at 39 000 r.p.m. for 18−20 h; 0.5 ml fractions were collected from top to bottom (fractions 1−24) and gD1−DAF was immunoprecipitated from all the fractions (Figure 5A and B). In MDCK cells, a considerable amount of gD1−DAF (40−50% of the total mature + immature forms) equilibrated at low density regions of the gradient (fractions 9−14, ~15−20% sucrose), although some of the protein was also present at the bottom of the gradient (Figure 5A). Note that fractions 17−24, representing the high density (soluble) material, contained mainly the immature form of gD1−DAF. This was in agreement with the results from the TX-100 extractions in the pulse−chased cells (Figure 2A), which also indicated that the ER form of gD1−DAF was soluble. In contrast, in FRT cells, the bulk of mature gD1−DAF (>85%) was recovered from fractions 17−24, near the bottom of the gradient, as expected for a soluble protein (Figure 5B). To confirm that all the protein had been solubilized, we analyzed the migration in the same gradient of two soluble transmembane proteins: gp114 in MDCK cells and Ag35/40kD in FRT cells. We found, as expected, that both remained in the bottom factions (17−24) of the gradient (Figure 5C and D). These results, together with the solubility data in Figure 3, suggest that either GPI-proteins and integral membrane proteins have different mechanisms for association with the apical sorting machinery, or that they use different vesicles for apical delivery (see Discussion).

We also studied the mobility of gD1−DAF in the same sucrose gradient in MDCK-ConA^r cells. In this experiment, we collected 1 ml fractions starting from the top of the gradient (fractions 1−12). As expected from the TX-100 extractability data, we found that gD1−DAF behaved in MDCK-ConA^r cells almost identically to MDCK cells (Figure 6). A fraction of gD1−DAF migrated in the low density part of the gradient, whilst most of the precursor protein remained at the bottom (Figure 6). In summary, a large fraction of the mature, Golgi form of gD1−DAF equilibrated at low density in MDCK and MDCK-ConA^r cells, whereas it did not migrate in FRT cells.

The equilibration of gD1−DAF at a low density region of the sucrose gradient in MDCK and MDCK-ConA^r cells suggested association of this protein with a lighter component. To examine whether GSLs co-migrated with gD1−DAF in the low density fraction of the sucrose gradient, we labeled MDCK and FRT cells overnight with [^{3}H]galactose and lysed them at 4°C in buffer containing 1% TX-100. After equilibrium centrifugation in a sucrose density gradient, 1 ml fractions were collected from the top to the bottom of the gradient (fractions 1−12). From each fraction the GSLs were extracted, separated on HPTLC and analyzed by densitometric scanning of the fluorographs. Figure 7, representative for two separate experiments, shows that the majority of the GSLs from both MDCK and FRT cells migrated to low density fractions. GSLs from MDCK cells accumulated mainly in one large peak in fractions 3−9 (~15−20% sucrose), predominantly overlapping with insoluble gD1−DAF (Figure 5A). GSLs from FRT cells also migrated to lower density fractions in a large peak (~16% sucrose), but comparison with Figure 5B indicates that there is only a minor amount (>10%) of insoluble gD1−DAF that equilibrates at the same isopycnic density. It is interesting to note that the GSL composition of the low density sucrose fractions equilibrating with insoluble gD1−DAF (fractions 2−7 for MDCK, and fractions 6−8 for FRT), was essentially similar to the composition of insoluble GSLs seen in Figure 4. In the same type of experiment, the bulk of the phospholipids from MDCK and FRT were found in the bottom fractions, at high densities, co-localizing with soluble gD1−DAF. However, as expected from its insolublity in TX-100, a substantial amount of endogenous SM did migrate to the same low density fractions as insoluble gD1−DAF (not shown). This confirms the

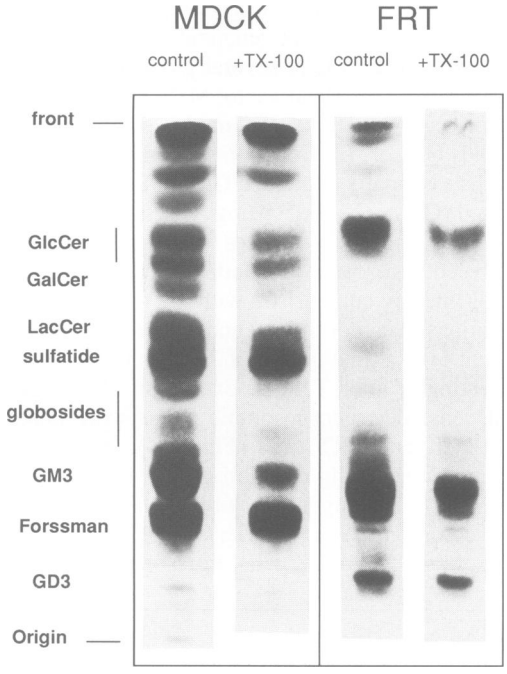

Fig. 4. Analysis of [^{3}H]galactose-labeled GSLs in MDCK and FRT cells, and their insolubility in TX-100. Confluent monolayers of MDCK and FRT cells were labeled overnight with [^{3}H]galactose as described in Materials and methods. Cells were incubated for 20 min at 4°C with either 1 ml TNE (control) or 1 ml TNE/TX-100 buffer (+TX-100) and GSLs were subsequently extracted from control cells and TX-100 lysates, and separated on HPTLC plates which were exposed to film for 4 days (MDCK) or 8 days (FRT). Radiolabeled GSLs were identified from their R_f values. GlcCer from MDCK cells and GM_3 from FRT migrated as double bands, probably due to fatty acid variations, and sometimes three products with unknown identity were found at the front on the HPTLC plate.

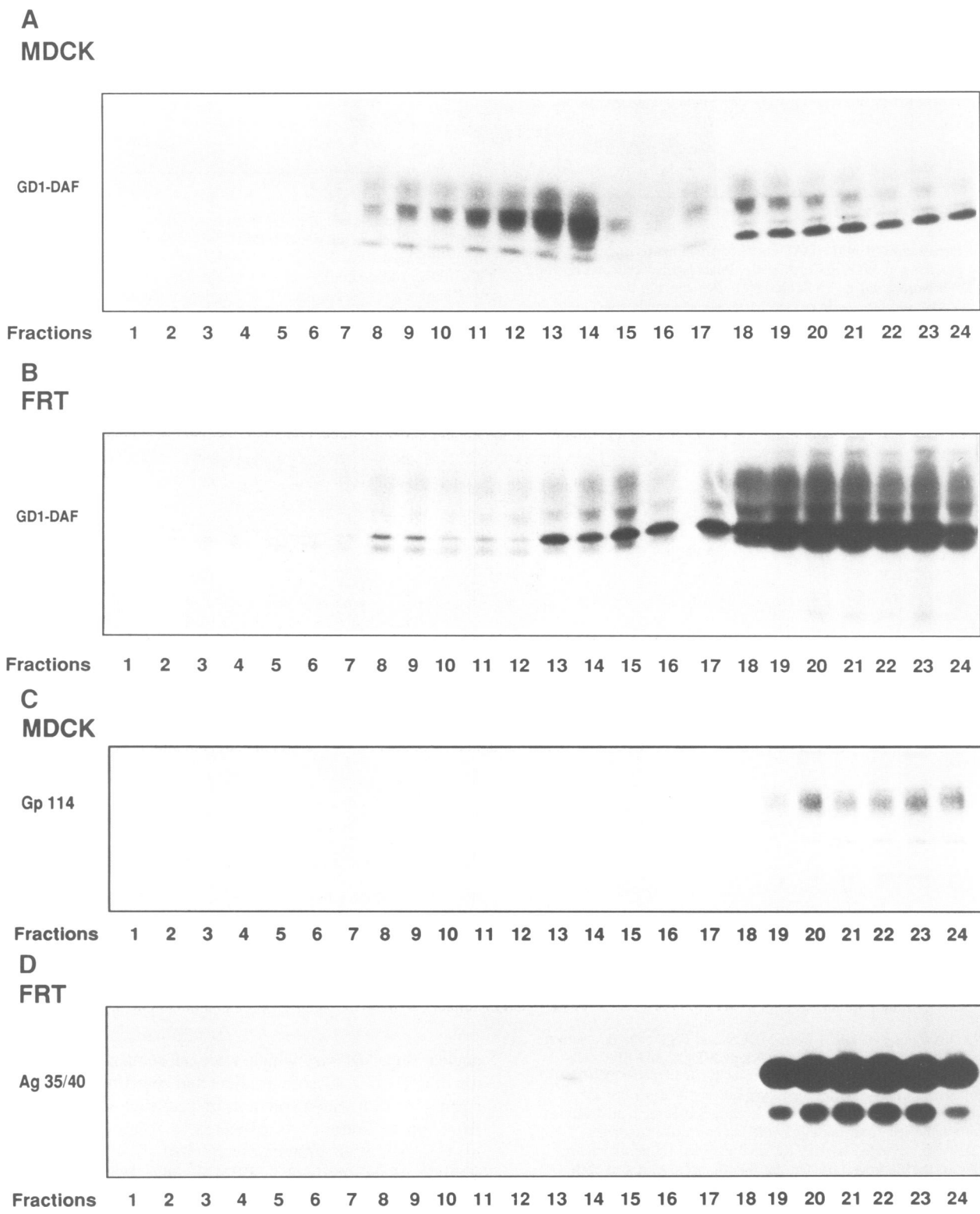

Fig. 5. Purification of gD1−DAF-enriched fractions on sucrose density gradients in MDCK and FRT cells. Pulse-labeled cells expressing gD1−DAF were lysed in TNE/TX-100 buffer and run through a linear 5−30% sucrose gradient. Fractions of 0.5 ml were collected from top to bottom after centrifugation to equilibrium and gD1−DAF was immunoprecipitated from all fractions. In MDCK cells (**A**), note the difference in molecular weight of the protein that is floating (mature form) relative to the immature form that remains at the bottom of the gradient. In FRT cells (**B**), both the mature and immature forms are restricted to the bottom fractions. Control experiments performed with two soluble proteins, gp 114 in MDCK (**C**) and Ag35/40kD in FRT cells (**D**), also showed recovery of both proteins only from the bottom fractions (17−24) of the gradients.

relationship between TX-100 insolubility and migration to low isopycnic densities in sucrose gradients for the various lipids.

These experiments suggested that in MDCK cells gD1−DAF associates with a fraction that is enriched with GSLs. Furthermore, the same enrichment of GSLs exists in a corresponding low density fraction from FRT cells but, in this case, it is devoid of gD1−DAF.

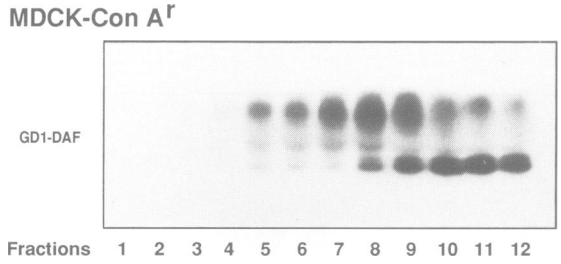

Fig. 6. Purification of gD1−DAF-enriched fractions on sucrose density gradients in MDCK-ConA^r cells. Pulse-labeled cells expressing gD1−DAF were lysed in TNE/TX-100 buffer and run through a linear 5−30% sucrose gradient (see Materials and methods). One milliliter fractions were collected from top to bottom after centrifugation to equilibrium and gD1−DAF was immunoprecipitated from all fractions.

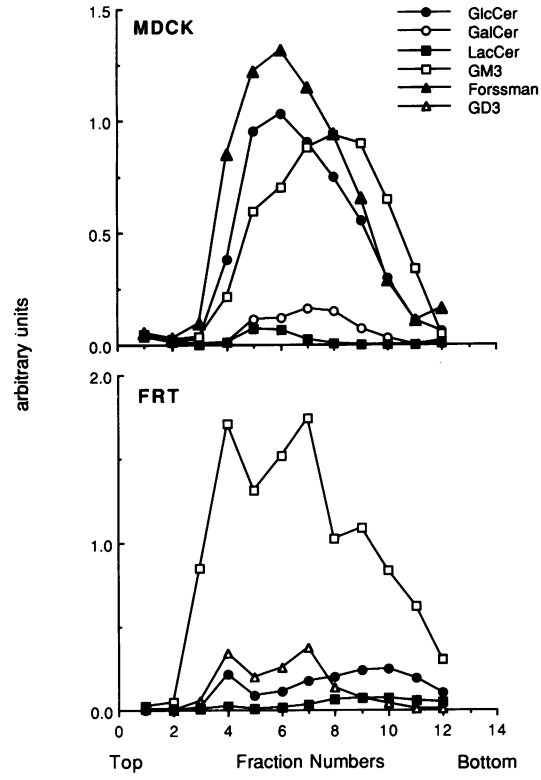

Fig. 7. Distribution of GSLs from MDCK and FRT cells on sucrose density gradients. Confluent monolayers of MDCK and FRT cells were labeled overnight with [^{3}H]galactose, lysed in TNE/TX-100 buffer, and applied to sucrose density gradients as described in Materials and methods. Labeled GSLs, extracted from 1 ml fractions that were collected from the top to the bottom of the gradients (1−12), were separated on HPTLC and analyzed by densitometric scanning of the fluorographs. On the fluorographs, GSLs in each fraction were scanned in an area of equal size, to allow for consistent correction for the background, which was measured in a control lane.

TX-100-insoluble pellets are membrane enriched in both MDCK and FRT cells

To test the hypothesis that gD1−DAF was associated with membrane structures in MDCK cells and to see if the same fractions existed in FRT cells, we isolated TX-100-insoluble residues using a recently published procedure (Garcia *et al.*, 1993). Both MDCK and FRT cells were again pulsed with [^{35}S]Met/Cys, incubated for 1 h in chase medium, and then collected. One percent TX-100 buffer was added to the post-

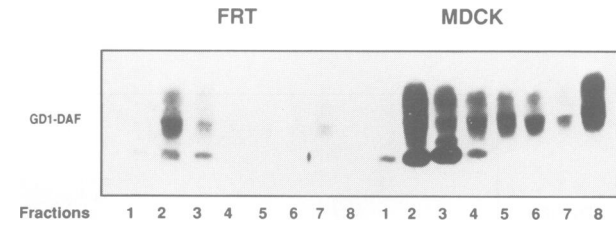

Fig. 8. Purification of gD1−DAF-enriched fractions on sucrose density gradients in FRT and MDCK cells. Post-nuclear supernatants from cells pulsed for 20 min and chased for 1 h were lysed with 1% TX-100 and loaded on 5−35% sucrose density gradients. gD1−DAF was immunoprecipitated from 1 ml fractions harvested from the top of the gradient. Note that the pellet, representing the TX-100-insoluble fraction, is enriched with gD1−DAF in MDCK cells, but not in FRT cells.

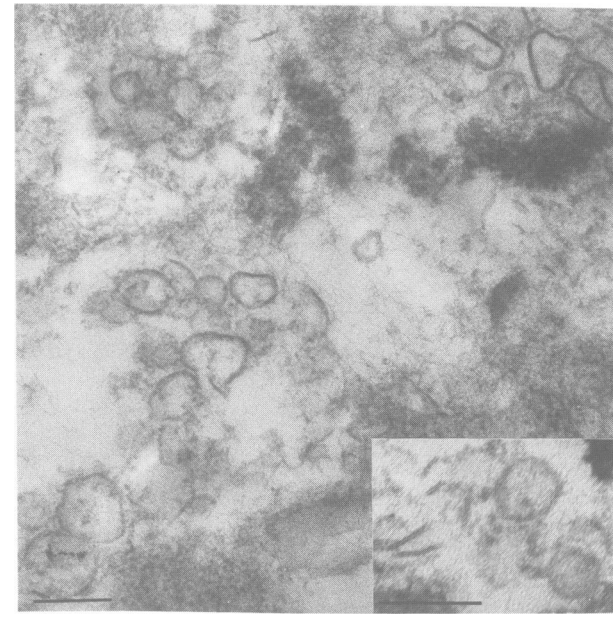

Fig. 9. TX-100-insoluble pellets from sucrose density gradient are enriched in membrane structures in both FRT and MDCK cells. Pellets from gradients shown in Figure 8 from MDCK (inset) and FRT cells were prepared for electron microscopy as described in Materials and methods. Note the presence of similar membrane structures in MDCK and FRT cells. Bar = 0.2 μm.

nuclear supernatants, which were subsequently loaded on top of a 5−35% sucrose gradient and centrifuged at 39 000 r.p.m. for 18 h. Eight fractions of 1 ml each were collected from top to bottom. As expected, a large percentage of gD1−DAF was immunoprecipitated from the bottom fraction of the gradient in MDCK cells, whilst there was almost nothing in the same fractions in FRT cells (Figure 8). To look at the structure of these insoluble pellets in MDCK and FRT cells, we analyzed them by electron microscopy (Figure 9). As previously shown for different cell lines (Brown and Rose, 1992; Garcia *et al.*, 1993), we observed layers of amorphous material together with a heterogeneous population of vesicles (~0.1−0.4 μm) and membrane fragments in both MDCK (Figure 9 inset) and FRT cells (Figure 9). Taken together, these experiments showed that the same kind of TX-100-insoluble membrane structure existed in both MDCK and FRT cells, but it associated with gD1−DAF only in MDCK cells (Figures 8 and 9).

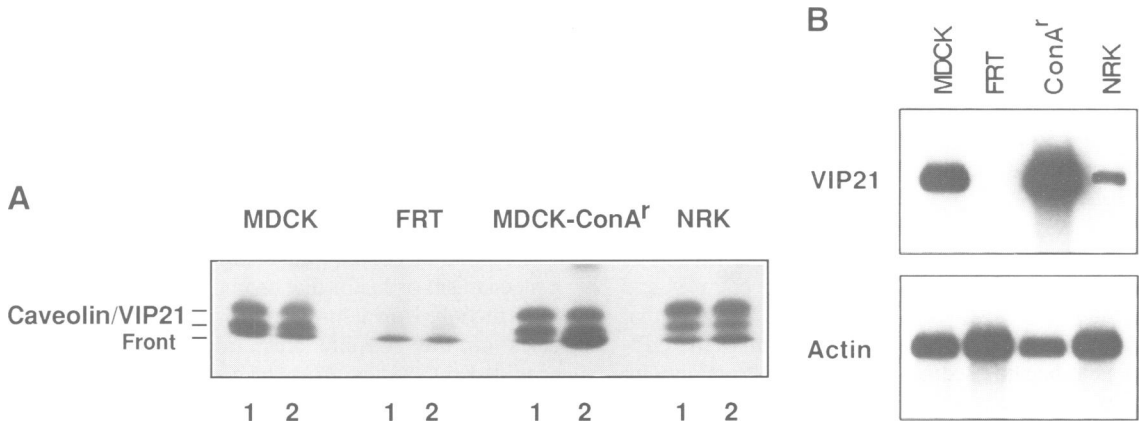

Fig. 10. Expression of VIP21/caveolin in MDCK, FRT, MDCK-ConA^r and NRK 49 F cells. (**A**) Immunoprecipitation. Steady-state metabolically labeled cells were immunoprecipitated with either the monoclonal antibody anti-caveolin (lanes 1) or the polyclonal VIP21-N antiserum (lanes 2). Both antibodies recognized the same doublet at 21–22 kDa in MDCK, MDCK-ConA^r and NRK cells, but not in FRT cells. (**B**) Northern blot analysis. mRNA isolated from MDCK (3 μg), FRT (6 μg), MDCK-ConA^r (3 μg) and NRK (6 μg) cells was run on a formaldehyde–agarose gel, transferred to nylon and hybridized to a ^{32}P-labeled MDCK VIP21 DNA probe derived from MDCK cells (Kurzchalia *et al.*, 1992). Actin was used as control. Note that even using double the quantity of mRNA we were not able to detect any caveolin messenger in FRT cells. In contrast, MDCK-ConA^r cells expressed an even higher level of VIP21 messenger with respect to MDCK. The reason for the lower signal in NRK cells (even when loading double amounts of RNA) could be related to probe specificity; in fact, the amount of the protein in the two cell lines is almost identical, as shown by the immunoprecipitation (A).

VIP21/caveolin is absent in FRT cells but is expressed in MDCK-ConA^r cells

The previous experiments led us to conclude that clusters of GPI-anchored proteins and GSLs existed in both MDCK and MDCK-ConA^r cells, but not in FRT cells. These clusters most likely form early in the Golgi and do not seem to be a sufficient signal for accurate sorting of GPI-proteins because they are present in both MDCK and MDCK-ConA^r cells, which display different polarity of gD1–DAF (Figure 1).

However, GPI-anchored proteins have been found to be enriched in caveolae. In addition, caveolin (or VIP21), a major protein component of these plasma membrane domains, has been found in both the apical and basolateral TGN-derived vesicles (Kurzchalia *et al.*, 1992) as well as in the TGN (Dupree *et al.*, 1993). These data strongly link the glycolipid/GPI-protein clusters with caveolae and suggest a functional relationship between them (Dupree *et al.*, 1993). We therefore investigated the presence of VIP21/caveolin in MDCK, FRT and MDCK-ConA^r cells. Cells were labeled overnight with [^{35}S]Met/Cys and VIP21/caveolin was immunoprecipitated using either a monoclonal or a polyclonal antibody (see Materials and methods). Surprisingly, we found that whereas MDCK-ConA^r cells and MDCK cells expressed large amounts of VIP21/caveolin, this protein was absent in FRT cells (Figure 10A). As a control for the specificity of the antibodies in rat cells, we showed that we could immunoprecipitate the protein from another rat cell line, NRK-49F (Figure 10A). Northern blot analysis of the mRNA extracted from MDCK, FRT, MDCK-ConA^r and NRK-49F cells did not detect any caveolin transcripts in FRT cells, thus confirming the immunoprecipitation data (Figure 10B). These data suggest that VIP21/caveolin could be one of the factors involved in the recruitment of GPI-proteins during transport to the surface. Although the lack of VIP21/caveolin in FRT cells might explain the solubility of gD1–DAF in TX-100, other adaptors would, however, be required for the sorting of GSL/GPI-protein patches because MDCK-ConA^r cells express VIP21/caveolin, but are unable to sort gD1–DAF.

Discussion

The cluster hypothesis

The 'cluster hypothesis' for the sorting of apical proteins via GSL rafts predicts specific interactions between apical proteins, GSLs and the TGN machinery for apical vesicle formation. Detergent insolubility has recently been used to assess the association of proteins with GSL rafts. Indeed, upon extraction of MDCK cells with the zwitterionic detergent CHAPS, the apical marker influenza HA was shown to form insoluble aggregates with GSLs and a group of characteristic membrane proteins (Kurzchalia *et al.*, 1992). That some of these proteins may be components of the apical sorting machinery was suggested by the observation that many of them were found in the CHAPS-insoluble residue after extraction of purified apical vesicles (Kurzchalia *et al.*, 1992). GPI-anchored proteins are depleted from CHAPS extracts (Fiedler *et al.*, 1993) but are co-enriched with GSLs and some of the the apical vesicular proteins in TX-100-insoluble aggregates (Fiedler *et al.*, 1993), suggesting that the interactions of the sorting machinery with GPI-anchored proteins are weaker than with influenza HA.

Whilst detergent insolubility provides an excellent tool to study the association of proteins and glycolipids, and to identify putative components of the apical sorting machinery, by itself, it does not provide a critical test for the role of this association. To gain insight into the functional significance of this process for the sorting of apical proteins in the TGN, we studied the existence and biochemical properties of detergent-insoluble aggregates of GPI-proteins and GSLs comparatively in MDCK cells and in two other epithelial cell lines that fail to sort GPI-proteins apically.

A GPI-anchored protein targeted basolaterally in FRT cells does not form TX-100-insoluble clusters

We examined the acquisition of detergent insolubility of gD1–DAF during biogenesis in both MDCK and FRT cells. The results with MDCK cells were in general agreement with those reported by Brown and Rose for the GPI-protein PLAP, i.e. a large fraction of gD1–DAF (~50%) became

detergent-insoluble at the time that it transited the Golgi apparatus (Figure 2A). However, we never observed the >90% insolubilization levels reported for PLAP (see Results). The insolubilization of gD1−DAF occurred much prior to reaching the TGN, i.e. before the glycoprotein received the carbohydrate modifications typical of medial and *trans* Golgi.

In striking contrast with its behavior in MDCK cells, gD1−DAF never became detergent-insoluble in FRT cells (Figure 2B). As it migrated along the secretory pathway and showed a similar change in electrophoretic mobility to that observed in MDCK cells, no significant fraction of the GPI-anchored protein became sedimentable after extraction with TX-100. Thus, mis-sorting of GPI-proteins to the basolateral surface in FRT cells correlated with lack of ability to cluster GPI-anchored proteins into TX-100-insoluble aggregates. These results suggest that clustering may be important for apical targeting of GPI-anchored proteins, but that it is not required for the basolateral targeting of these proteins in FRT cells.

Basolateral glycosphingolipid sorting in FRT cells

FRT cells displayed yet another striking difference with MDCK cells: they preferentially delivered C6-NBD-GlcCer to the basolateral surface with a 2-fold enrichment relative to C6-NBD-SM (Table I). This is exactly the reverse of what had been previously observed in MDCK and Caco-2 cells (van't Hof *et al.*, 1992). Our results suggest that GSLs may be concentrated in the basolateral membranes of FRT cells. We hypothesize that, since the apical surface of thyroid cells *in vivo* does not face an unusually harsh environment, evolution may not have favored the concentration of GSLs there. However, the apical/basolateral polarity of GSLs has yet to be determined in primary thyroid cells. Still, the observations reported here validate the use of fluorescent NBD-sphingolipids and prove that this type of assay is capable of detecting cell type-specific lipid-sorting events.

We explored the possibility that the reversed polarity of GSLs in FRT cells might originate from the expression of a different set of GSLs with a decreased ability to form clusters. Indeed, as detected by labeling of GSLs with [^{3}H]galactose (Saito *et al.*, 1984; van Echten and Sandhoff, 1989), FRT cells express a GSL pattern different from that observed in MDCK cells (Figure 4), with some common glycolipids (GlcCer and GM_3), a general reduction in galactose-containing GSLs (GalCer, LacCer, Forssman antigen and sulfatide) and the expression of GD_3, which is absent in MDCK cells. Similar patterns for cold and [^{3}H]galactose-labeled GSLs as those reported here in MDCK (Figure 4) have been observed before (Hansson *et al.*, 1986; Nichols *et al.*, 1988). Both common and cell-line specific GSLs show an overall similar insolubility in TX-100 (Figure 4). For the common glycolipids, GlcCer is 40% insoluble and GM_3 50%. MDCK-specific Forssman antigen is 75% insoluble, the cerebrosides 25−35% and sulfatide 50%; FRT-specific GD_3 is 40% insoluble in TX-100. From this, we can conclude that GSL clustering, as measured by detergent insolubility, does still occur in FRT cells.

Sucrose density gradient analysis of GSL clusters from FRT and MDCK cells showed that they peaked at the same isopycnic density. In agreement with the results described above, gD1−DAF co-migrated with the GSL peak in MDCK cells, but in FRT cells it remained at the bottom of the gradient, fully separated from the insoluble GSLs. These results suggest that GPI-anchored proteins are sorted to the basolateral membrane independently of GSL patches. They also show that the clustering of GSLs does not function, by itself, as an apical sorting signal.

VIP21/caveolin is absent in FRT cells and may be the clustering factor

The results discussed above suggested that FRT cells lack a mechanism or factor that promotes clustering of GSLs and GPI-anchored proteins prior to reaching the TGN. Some clues on the possible clustering mechanism have been provided by studies on surface caveolae. These structures are enriched in both GSLs and GPI-anchored proteins (Rothberg *et al.*, 1990; Anderson *et al.*, 1992) and contain >90% of surface caveolin (Dupree *et al.*, 1993). Since this protein is also found in the Golgi apparatus, as well as in apical and basolateral vesicles, where it has been named VIP21, we looked for VIP21/caveolin in both MDCK and FRT cells. We found that, whereas VIP21/caveolin was expressed at high levels in MDCK cells (as previously shown), FRT cells did not express this protein and, furthermore, its mRNA was also absent (Figure 10). These results suggest that VIP21/caveolin may be directly involved in the clustering of GPI-anchored proteins and GSLs in MDCK cells. Consequently, its absence from FRT cells may be responsible for the lack of interaction between GPI-anchored proteins and GSLs. This interaction may be essential for apical sorting in the TGN, perhaps by allowing the recruitment of components of the apical machinery (see below). However, our experiments do not exclude additional causes for defective association of GPI-protein and GSL clusters, e.g. different GPI structures or different GSL compositions in FRT and MDCK cells, or alteration of the luminal pH of the TGN in FRT cells. Reconstitution of VIP21/caveolin expression in FRT cells by transfection of its cDNA (experiments in progress) will help to elucidate this important point.

A ConA^r mutant of MDCK cells unable to sort GPI-anchored proteins delivers GSLs to the apical domain and expresses normal levels of VIP21/caveolin

Having found that VIP21/caveolin was most likely necessary for clustering of GPI-anchored proteins and GSLs, we explored whether it was sufficient for their apical sorting. We have previously shown that a ConA^r mutant of MDCK cells (Green *et al.*, 1981; Meiss *et al.*, 1982), displays an unpolarized distribution of both endogenous (Lisanti *et al.*, 1990a) and transfected (Hannan *et al.*, 1993) GPI-anchored proteins. We show here (Figure 1) that gD1−DAF was targeted without polarity to the cell surface from the TGN in MDCK-ConA^r cells, which explains its unpolarized surface distribution. Interestingly, the apical delivery of C6-NBD-GlcCer was unchanged, relative to the parental line (Table I). Furthermore, the TX-100-insoluble fraction of gD1−DAF, although somewhat less than in wild-type MDCK cells (~35% compared with 45%), was still considerable, and equilibrated at a similar isopycnic density as the corresponding fraction in MDCK cells (Figure 6). In agreement with the hypothesis that VIP21/caveolin might be a clustering factor, we found that it was expressed at wild-type levels in MDCK-ConA^r cells (Figure 10). These results indicated that the ConA^r mutation did not affect the

ability of GPI proteins to cluster with GSLs as much as it affected their sorting. This conclusion is supported by the biophysical experiments of Hannan *et al.* (1993) (see Introduction), which indicated that the GPI-anchored proteins recently arrived at the apical cell surface were clustered in ConA^r cells (as in wild-type cells), but were not immobilized, presumably because of defective interactions with the sorting machinery.

Since VIP21/caveolin is not glycosylated, its structure should not be altered in ConA^r cells and, therefore, cannot be responsible for the reduced sorting ability of this cell line. This conclusion is also supported by the presence of VIP21 in both apical and basolateral post-TGN carrier vesicles (Kurzchalia *et al.*, 1992). A more likely possibility is the alteration of a lectin-like luminal factor, important for apical sorting (sorting receptor), which links the clusters to the apical vesicle-forming machinery. A third alternative is that the ConA^r mutation changes the intra-Golgi environment (e.g. pH), leading to defective interaction of the clusters with the sorting machinery. Taken together, the targeting phenotypes of MDCK-ConA^r and FRT cells, and their differences in the expression of VIP21/caveolin, imply that this protein may be necessary, but not sufficient, for the apical sorting of GSLs and GPI-anchored proteins.

VIP21/caveolin, clustering and sorting of apical proteins

The experiments described in this report provide important insights into the operation of the apical sorting machinery of epithelial cells. Namely, (i) they support the 'cluster hypothesis' because the disruption of the association between GPI-anchored proteins and GSLs in FRT cells leads to reversed, basolateral delivery of both components, (ii) they provide intriguing evidence for VIP21/caveolin as a key factor in the association of GSLs with GPI-anchored proteins, because VIP21/caveolin is not expressed in FRT cells, and (iii) they show that clustering with GSLs, although necessary for apical sorting, may not be sufficient, because GPI-anchored proteins appear to be unsorted in MDCK-ConA^r cells, suggesting the existence of additional components of the cluster that are necessary for attachment to the apical vesicle-forming machinery. A dilemma presented by these experiments is why the apical polarity of integral membrane proteins, such as DPPIV (Zurzolo *et al.*, 1992a) and influenza HA (Zurzolo *et al.*, 1992b), is not affected by the defect that reverses GPI-protein distribution in FRT cells. Possible answers to this question may be related to the differential detergent insolubility of GPI proteins and integral membrane proteins. Similar putative components of the apical sorting machinery are found in CHAPS- and TX-100-insoluble residues, although they are found in different relative amounts. Furthermore, GPI-anchored proteins and integral membrane proteins show different susceptibility to solubilization by these detergents (Brown and Rose, 1992; Kurzchalia *et al.*, 1992; Fiedler *et al.*, 1993; Garcia *et al.*, 1993; and data from this report in Figure 3). CHAPS dissociates GPI-anchored proteins from the putative apical sorting machinery, but TX-100 appears to preserve this interaction. This suggests that different factors, with different sensitivity to detergents, mediate association of GPI-anchored proteins and integral membrane proteins with the apical sorting machinery. This variability may be a function of different regulatory proteins involved in the clustering event. In this regard, it is interesting to note that certain cytoplasmically localized protein kinases have been found clustered with GPI-anchored proteins and integral membrane proteins at the cell surface in lymphocytes, and that this association leads to specific signaling events (Stefanova *et al.*, 1991; Cinek and Horejsi, 1992; Thomas and Samelson, 1992). Cell-specific variability in the expression of these regulatory factors may also explain the variable targeting of integral membrane proteins in different epithelial cell types. The identification of the different components of the sorting machinery and characterization of their specific roles appears to be the only possible solution to many of these questions.

Materials and methods

Materials

Sulfo NHS derivatives were from Pierce (Rockford, IL), rabbit antibody (Ig fraction) against herpes simplex virus (HSV) was from Dakopatt, monoclonal anti-caveolin antibody (clone 2234, IgG1) was from Transduction Laboratories (Lexington, KY). The polyclonal rabbit antiserum anti-N terminus VIP21 peptide and the VIP21 cDNA from MDCK cells were kind gifts from Paul Dupree (EMBL).

Cells and culture conditions

FRT, MDCK II and MDCK-ConA^r cells stably expressing gD1−DAF have been described previously (Lisanti *et al.*, 1989; Hannan *et al.*, 1993; Zurzolo *et al.*, 1993). FRT cells were grown in F12 Coons modified medium containing 5% fetal calf serum (FCS). MDCK, MDCK-ConA^r and NRK 49F were maintained in DMEM supplemented with 10% FCS.

Cell surface delivery of gD1 − DAF

To follow the appearance of newly synthesized gD1−DAF at the cell surface, we modified a protocol previously described for MDCK cells (Lisanti *et al.*, 1990b). Briefly, cell surface free amino groups were quenched with 1 ml of sulfo-SHPP [0.5 mg/ml in ice-cold phosphate-buffered saline (PBS)-C/M] added to both the apical and the basolateral compartments (repeated 5 times, 15 min each). The appearance of new free surface amino groups, following incubation at 37°C with pre-warmed normal medium, was monitored by domain-selective labeling with sulfo-NHS-biotin (Sargiacomo *et al.*, 1989). Filters were then excised from the chamber and subjected to lysis and immunoprecipitation (Le Bivic *et al.*, 1989). After SDS−PAGE and transfer to nitrocellulose, biotinylated proteins were detected by blotting with [^{125}I]streptavidin.

C6-NBD-sphingolipid transport assay

Delivery of C6-NBD-sphingolipids to the cell surface was assayed as before (van't Hof *et al.*, 1992; van Meer and van't Hof, 1993). Briefly, the fluorescent precursor C6-NBD-ceramide was incorporated into filter-grown epithelial cells by exchange from unilamellar phosphatidylcholine liposomes for 30 min at 10°C. Delivery to the cell surface of intracellularly synthesized C6-NBD-glucosylceramide (C6-NBD-GlcCer) and C6-NBD-sphingomyelin (C6-NBD-SM) was assayed for 1 h at 37°C, by continuous depletion by using BSA (1% w/v in HBSS) in the apical and basolateral media, followed by one back-exchange against HBSS + BSA for 30 min at 10°C to optimize depletion. Fluorescent lipids were extracted from the combined apical media, the combined basal media and the cell monolayer on the filter, after which they were quantitatively analyzed by HPTLC and measurement of NBD-fluorescence in the individual lipid spots (van Meer *et al.*, 1987; van't Hof and van Meer, 1990).

Lipid analysis

Phospholipids were analyzed by extraction according to Bligh and Dyer (1959), followed by separation by two-dimensional HPTLC, localization by iodine staining, and quantitation according to Rouser *et al.* (1970). Cellular GSLs were studied after labeling for 12−16 h with [^{3}H]galactose (5 μCi/ml) in glucose-free medium supplemented with 5% dialyzed serum, 20 mM HEPES (pH 7.4) and 0.5 mg/ml glucose (Nichols *et al.*, 1988; van Echten and Sandhoff, 1989). GSLs were extracted according to Folch *et al.* (1957) or Bligh and Dyer (1959). These two-phase systems were used to separate lipids in the organic phase from salts, detergent and sucrose in the water phase, which will otherwise interfere with lipid separation on HPTLC. To minimize loss of GSLs in the water phases, these were first

washed one or two times with $CHCl_3$/MeOH (2:1) that was added to the organic lipid extract. Secondly, remaining GSLs in the water phases were isolated using Sep-Pak C18 cartridges and added to the total lipid extract. GSLs were separated on HPTLC by development in $CHCl_3$/MeOH/0.2% $CaCl_2$ (60:35:8; v/v) and the relative labeling of different GSLs was determined by fluorography and densitometric scanning of the fluorographs. Labeled GSLs were identified from their R_f values (van Echten and Sandhoff, 1989).

Pulse–chase and TX-100 extraction

TX-100 extractability during pulse–chase experiments was assayed as described before (Brown and Rose, 1992). Briefly, cells that had just reached confluency in 35 mm dishes were stimulated overnight with Na butyrate at a final concentration of 10 mM. Cells were then starved of methionine and cysteine for 20 min, and pulse labeled for 5 min with 100 μl of pulsing medium containing ~500 μCi/ml of trans ^{35}S label and then incubated in chase medium (DME containing 10% FCS and 100 × Met and Cys) for different times. After each time point, cells were washed twice with PBS on ice as described before (Skibbens *et al.*, 1989), lysed for 20 min on ice in 1 ml of TNE/TX-100 buffer [25 mM Tris–HCl (pH 7.5), 150 mM NaCl, 5 mM EDTA, 1% TX-100 + a cocktail of protease inhibitors (Lisanti *et al.*, 1988)]. Lysates were collected and centrifuged at 13 000 r.p.m. for 2 min at 4°C. Supernatants, representing the soluble material, were removed and pellets were solubilized in 100 μl of solubilization buffer [50 mM Tris–HCl (pH 8.8), 5 mM EDTA, 1% SDS] and the DNA was sheared through a needle of 22g. Both soluble and insoluble materials were adjusted to 0.1% SDS before immunoprecipitation with specific antibodies, as previously described (Le Bivic *et al.*, 1989).

Sucrose gradients

Sucrose gradient analysis of TX-100-insoluble residue was performed following two recently published protocols (Brown and Rose, 1992; Garcia *et al.*, 1993). (i) Cells were grown to confluency in 10 cm dishes and two dishes were used for each gradient. For gD1–DAF, gD1–DAF-expressing cells were induced overnight with 10 mM Na butyrate, labeled for 15 min with 500 μCi/ml of [^{35}S]Met/Cys and incubated in chase medium for 1 h. This time was chosen in order to catch the proteins in the process of reaching the plasma membrane. Monolayers were then rinsed in PBS and lysed for 20 min in TNE/TX-100 buffer on ice. Lysates were scraped from the dish and brought to 40% sucrose, and placed at the bottom of a centrifuge tube. A linear sucrose gradient (5–30% in TNE) was layered on top of the lysates and centrifuged at 39 000 r.p.m. for 18–20 h in a Beckman SW41 rotor. Fractions of 0.5 or 1 ml were harvested from the top of the gradient using a pump (Bucher, Autodensity-flow). Immunoprecipitation of gD1–DAF and other antigens was performed on the different fractions that were brought to ~20% sucrose and to 1% TX-100. (ii) Cells grown to confluency on 10 cm dishes were rinsed twice with PBS on ice, scraped in 1 ml TNE buffer and broken by passage through a 23 g needle. Post-nuclear supernatants were brought to 1% TX-100 and lysed for 10 min at 4°C. Lysates were loaded on top of a 5–30% sucrose gradient in TNE/0.5% TX-100 and centrifuged at 39 000 r.p.m. for 18 h in a Beckman SW41 rotor. One milliliter fractions were harvested from the top, pellets of the gradients (fraction 8 in Figure 9) were solubilized in 1% SDS buffer, brought to 0.1% SDS and subjected to immunoprecipitation together with the other fractions.

Electron microscopy

To analyze the TX-100-insoluble fraction, pellets from gradients (no. 2) were rinsed in 0.1 M cacodylate buffer, fixed in 3% glutaraldehyde and processed for transmission electron microscopy following a standard protocol (Rodriguez-Boulan, 1983).

Steady-state metabolic labeling and caveolin immunoprecipitation

After washing confuent monolayers with starvation medium (DME lacking Met and Cys, 0.2% BSA and 10 mM HEPES), cells were incubated overnight in the same medium containing 100 μCi/ml of [^{35}S]Met/Cys. The cells were then scraped in lysis buffer and caveolin was immunoprecipitated using either a monoclonal antibody (Transduction Laboratories) or a polyclonal rabbit serum against an N terminal (residues 14–33) peptide of VIP21 (Dupree *et al.*, 1993) following a standard protocol (Le Bivic *et al.*, 1989).

Northern blot analysis of caveolin expression

Three confluent monolayers from 150 mm dishes were used to prepare mRNA via oligo(dT)–cellulose affinity cromatography (Stratagene) following a standard protocol (Maniatis *et al.*, 1982). Purified mRNA samples (3–6 μg) were run on formaldehyde–agarose gels and blotted to Duralon-UV nylon membranes (Stratagene) according to Bowler *et al.* (1989). Membranes were probed with random-primed ^{32}P-labeled DNA fragments of MDCK VIP21 cDNA (Kurzchalia *et al.*, 1992) or human actin according to standard procedures (Amersham).

Acknowledgements

We are indebted to Dr P.Dupree for his generous gifts of VIP21-N antiserum and cDNA, and for stimulating discussion. We also thank Mrs L.Cohen-Gould for the electron microscopy assistance, and Misses L.Van Houten and J.Hornung for photographic reproductions. C.Z. is particularly grateful to Dr Neuhaus on keyboards and mouse, and to Drs Gilmartin and Bowler for backing support. This work was supported by National Institutes of Health grants GM34107 and GM41771 to E.R.B. C.Z. is also supported by the Italian MURST (Ministero Università e Ricerca Scientifica e Tecnologica). W.H. is the recipient of a New York Heart Association Participating Laboratory Fellowship.

References

Ali,N. and Evans,W.H. (1990) *Biochem. J.*, **271**, 193–199.
Anderson,R.G.W., Kamen,B.A., Rothberg,K.G. and Lacey,S.W. (1992) *Science*, **255**, 410–411.
Bligh,E.G. and Dyer,W.J. (1959) *Can. J. Biochem. Physiol.*, **37**, 911–917.
Bowler,C., Alliotte,T., De loose,M., Van Montagu,M. and Inze,D. (1989) *EMBO J.*, **8**, 31–38.
Brown,D.A. (1992) *Trends Cell Biol.*, **2**, 338–343.
Brown,D.A. and Rose,J.K. (1992) *Cell*, **68**, 533–544.
Brown,D.A., Crise,B. and Rose,J.K. (1989) *Science*, **245**, 1499–1501.
Cinek,T. and Horejsi,V. (1992) *J. Immunol.*, **149**, 2262–2270.
Cross,G.A.M. (1990) *Annu. Rev. Cell Biol.*, **6**, 1–39.
Dupree,P., Parton,R.G., Raposo,G., Kurzchalia,T.V. and Simons,K. (1993) *EMBO J.*, **12**, 1597–1605.
Ferguson,M.A.J. and Williams,A.F. (1988) *Annu. Rev. Biochem.*, **57**, 285–320.
Fiedler,K., Kobayashi,T., Kurzchalia,T.V. and Simons,K. (1993) *Biochemistry*, **32**, 6365–6373.
Folch,J.,' Lees,M. and Stanley,G.H.S. (1957) *J. Biol. Chem.*, **226**, 497–509.
Futerman,A.H., Stieger,B., Hubbard,A.L. and Pagano,R.E. (1990) *J. Biol. Chem.*, **265**, 8650–8657.
Garcia,M., Mirre,C., Quaroni,A., Reggio,H. and Le Bivic,A. (1993) *J. Cell Sci.*, **104**, 1281–1290.
Green,R.F., Meiss,H.K. and Rodriguez-Boulan,E. (1981) *J. Cell Biol.*, **89**, 230–239.
Hannan,L.A., Lisanti,M.P., Rodriguez-Boulan,E. and Edidin,M. (1993) *J. Cell Biol.*, **120**, 353–358.
Hansson,G.C., Simons,K. and van Meer,G. (1986) *EMBO J.*, **5**, 483–489.
Hoessli,D. and Rungger-Brandle,E. (1985) *Exp. Cell Res.*, **156**, 239–250.
Hooper,N.M. and Turner,A.J. (1988) *Biochem. J.*, **250**, 865–869.
Jeckel,D., Karrenbauer,A., Birk,R., Schmidt,R.R. and Wieland,F. (1990) *FEBS Lett.*, **261**, 155–157.
Kurzchalia,T.V., Dupree,P., Parton,R.G., Kellner,R., Virta,H., Lehnert,M. and Simons,K. (1992) *J. Cell Biol.*, **118**, 1003–1014.
Le Bivic,A., Real,F.X. and Rodriguez-Boulan,E. (1989) *Proc. Natl Acad. Sci. USA*, **86**, 9313–9317.
Le Bivic,A., Sambuy,Y., Mostov,K. and Rodriguez-Boulan,E. (1990) *J. Cell Biol.*, **110**, 1533–1539.
Lisanti,M. and Rodriguez-Boulan,E. (1990) *Trends Biochem. Sci.*, **15** 113–118.
Lisanti,M., Sargiacomo,M., Graeve,L., Saltiel,A. and Rodriguez-Boulan,E. (1988) *Proc. Natl Acad. Sci. USA*, **85**, 9557–9561.
Lisanti,M., Caras,I.P., Davitz,M.A. and Rodriguez-Boulan,E. (1989) *J. Cell Biol.*, **109**, 2145–2156.
Lisanti,M.P., Le Bivic,A., Saltiel,A. and Rodriguez-Boulan,E. (1990a) *J. Memb. Biol.*, **113**, 155–167.
Lisanti,M.P., Caras,I.W., Gilbert,T., Hanzel,D. and Rodriguez-Boulan,E. (1990b) *Proc. Natl Acad. Sci. USA*, **87**, 7419–7423.
Low,M.G. and Saltiel,A.R. (1988) *Science*, **239**, 268–275.
Maniatis,T., Fritsch,E.F. and Sambrook,J. (1982) *Molecular Cloning: A Laboratory Manual*. Cold Spring Harbor Laboratory Press, Cold Spring Harbor, NY.
Meiss,H.K., Green,R.F. and Rodriguez-Boulan,E. (1982) *Mol. Cell Biol.*, **2**, 1287–1294.

Nichols,G.E., Shiraishi,T. and Young,W.W.,Jr (1988) *J. Lipid Res.*, **29**, 1205–1213.
Ojakian,G.K. and Schwimmer,R. (1988) *J. Cell Biol.*, **107**, 2377–2378.
Powell,S.K., Cunningham,B.A., Edelman,G.M. and Rodriguez-Boulan,E. (1991) *Nature*, **353**, 76–77.
Rodriguez-Boulan,E. (1983) *Methods Enzymol.*, **98**, 486–501.
Rodriguez-Boulan,E. and Nelson,W.J. (1989) *Science*, **245**, 718–725.
Rodriguez-Boulan,E. and Powell,S.K. (1992) *Annu. Rev. Cell Biol.*, **8**, 395–427.
Rothberg,K.G., Ying,Y.-S., Kamen,B.A. and Anderson,R.G.W. (1990) *J. Cell Biol.*, **111**, 2931–2938.
Rothberg,K.G., Heuser,J.E., Donzell,W.C., Ying,Y.-S., Glenney,J.R. and Anderson,R.G.W. (1992) *Cell*, **68**, 673–682.
Rouser,G., Fleischer,S. and Yamamoto,A. (1970) *Lipids*, **5**, 494–496.
Saito,M., Saito,M. and Rosenberg,A. (1984) *Biochemistry*, **24**, 3045–3059.
Sargiacomo,M., Lisanti,M., Graeve,L., Le Bivic,A. and Rodriguez-Boulan,E. (1989) *J. Memb. Biol.*, **107**, 277–286.
Simons,K. and van Meer,G. (1988) *Biochemistry*, **27**, 6197–6202.
Simons,K. and Wandinger-Ness,A. (1990) *Cell*, **62**, 207–210.
Skibbens,J.E., Roth,M.G. and Matlin,K.S. (1989) *J. Cell Biol.*, **108**, 821–832.
Stefanova,I., Horejsi,V., Ansotegui,I.J., Knapp,W. and Stockinger,H. (1991) *Science*, **254**, 1016–1019.
Thomas,P.M. and Samelson,L.E. (1992) *J. Biol. Chem.*, **267**, 12317–12322.
Thompson,T.E. and Tillack,T.W. (1985) *Annu. Rev. Biophys. Biophys. Chem.*, **14**, 361–386.
van Echten,G. and Sandhoff,K. (1989) *J. Neurochem.*, **52**, 207–214.
van Meer,G. (1989) *Annu. Rev. Cell Biol.*, **5**, 247–275.
van Meer,G. (1993) *Curr. Opin. Cell Biol.*, (1993) **5**, 661–673.
van Meer,G. and Burger,K.N.J. (1992) *Trends Cell Biol.*, **2**, 332–337.
van Meer,G. and Simons,K. (1988) *J. Cell Biochem.*, **36**, 51–58.
van Meer,G. and van't Hof,W. (1993) *J. Cell Sci.*, **104**, 833–842.
van Meer,G., Stelzer,E.H., Wijnaendts van Resandt,R.W. and Simons,K. (1987) *J. Cell Biol.*, **105**, 1623–1635.
van't Hof,W. and van Meer,G. (1990) *J. Cell Biol.*, **111**, 977–986.
van't Hof,W., Silvius,J., Wieland,F. and van Meer,G. (1992) *Biochem. J.*, **283**, 913–917.
Wilson,J.M., Fasel,N. and Kraehenbuhl,J.-P. (1990) *J. Cell Sci.*, **96**, 143–149.
Zurzolo,C. and Rodriguez-Boulan,E. (1993) *Science*, **260**, 550–552.
Zurzolo,C., Le Bivic,A., Quaroni,A., Nitsch,L. and Rodriguez-Boulan,E. (1992a) *EMBO J.*, **11**, 2337–2344
Zurzolo,C., Polistina,C., Saini,M., Gentile,R., Migliaccio,G., Bonatti,S. and Nitsch,L. (1992b) *J. Cell Biol.*, **117**, 551–564.
Zurzolo,C., Lisanti,M.P., Caras,I.W., Nitsch,L. and Rodriguez-Boulan,E. (1993) *J. Cell Biol.*, **121**, 1031–1039.

Received on August 13, 1993; revised on October 1, 1993